

## Oscillatory Paramagnetic Magneto-Optical Kerr Effect in Ru Wedges on Co

A. Carl and D. Weller

IBM Research Division, Almaden Research Center, 650 Harry Road, San Jose, California 95120

(Received 5 August 1994)

Sharp, quantum-well-like resonances in the field dependent polar magneto-optical Kerr effect of evaporated Ru wedges on perpendicularly magnetized Co as a function of the Ru thickness are reported. This effect selectively measures free electronic excitations in Ru and is, via the Pauli paramagnetic susceptibility, proportional to the free electron density of states at the Fermi level. A peak separation of 1.2 nm agrees with long period indirect magnetic exchange coupling oscillations in perpendicular Co/Ru-wedge/Co sandwiches.

PACS numbers: 75.50.Rr, 73.20.Dx, 75.30.Et, 78.20.Ls

The magneto-optical Kerr effect (MOKE) has attracted much attention recently as a sensitive method to investigate quantum confinement effects in ultrathin ferromagnetic (FM) films, like fcc-Fe(100) sandwiched between Au [1]. Oscillations in the MOKE amplitude in fcc-Fe(100) films spaced by noble metal (NM) layers like Cu [2] and Au or Ag [3,4] as a function of the NM spacer thickness have been discovered and viewed in conjunction with the formation of spin polarized quantum well states. These MOKE experiments were carried out in air on structures capped with 60 atomic layers (AL) of Cu(100) [2] or 10 AL of Au(100) [3,4] and demonstrated the extreme sensitivity of MOKE to subtle electronic structure features. Periodicities of  $\sim 5$  AL consistent with indirect magnetic exchange coupling oscillation periods in FM/NM/FM structures were found [2,4]. Such oscillations had been observed before in many different experiments in polycrystalline (111) textured [5,6] and epitaxial (001) [7], (110) [8], and (111) [9,10] oriented multilayers and sandwiches and have attracted much theoretical and experimental interest. Current theories emphasize the importance of free electrons at the Fermi surface in RKKY and quantum well models to explain these phenomena [11–15]. Therefore, experiments probing the electronic structure at or near the Fermi level,  $\epsilon_F$ , provide the most critical information about the electronic origin of exchange coupling across nonmagnetic spacers. Examples of such experiments are inverse [16] and direct [17] photoemission spectroscopy, which have probed the  $\mathbf{k}$ -point dependent electronic density of states,  $N(\epsilon_F, \mathbf{k})$ , in NM/FM overlayer systems and have established their relationship with long period coupling oscillations.

In this Letter, we exploit the high sensitivity of MOKE to devise a *new* experiment, which selectively probes *free* electrons in NM spacers or overlayers. It is based on the idea that *field-induced* MOKE is related to the paramagnetic susceptibility, which for Pauli paramagnets is directly proportional to the  $\mathbf{k}$ -space integrated free electron density of states at the Fermi level,  $N(\epsilon_F)$ . Paramagnetic Kerr effects are known to be fairly large, e.g., of the order of several millidegrees per tesla in thick Ag, Au, or

Cu films [18,19] and should therefore be detectable in ultrathin NM films with a high resolution MOKE setup. Because of their linear external field dependence, these effects should furthermore be separable from field independent ferromagnetic contributions. We demonstrate here that sharp  $N(\epsilon_F)$  resonances can be observed in NM/FM overlayer structures by using field dependent Kerr measurements. We find peak separations of  $\sim 1.2$  nm which agree with long period coupling oscillations in exchange for coupled FM/NM/FM sandwich structures. We also resolve much shorter period fine structure of order 0.1–0.3 nm, which might challenge current theories [11–15].

Our experimental results are demonstrated for a (0001) oriented Ru wedge on a 3 AL thick hexagonal Co film with perpendicular magnetic anisotropy. The samples were grown in a  $10^{-9}$  mbar electron beam evaporator system on 1 in. diam fused silica substrates. The substrates were cleaned *ex situ* with a standard degreasing procedure and subsequently preheated to  $\sim 450^\circ\text{C}$  in vacuum before a 20 nm thick Pt base layer was deposited at  $\sim 400^\circ\text{C}$  at a rate of  $\sim 0.1$  nm/s. After cooling the substrates to ambient temperature ( $\sim 40^\circ\text{C}$ ), a nominally 0.6 nm (3 AL) thick Co film was deposited, followed by a continuous linear Ru wedge covering thicknesses between 0.1 and 2 nm using a moving shutter technique [24], and the structure was completed with a 2 nm Au protective layer. The Pt buffer serves as a high quality fcc (111) seed layer for the growth of Co. Typical terrace widths between 15 and 30 nm and a dispersion angle of  $\sim 5^\circ$  of the Pt buffer are concluded from high resolution transmission electron microscopy [20] and synchrotron-based x-ray diffraction studies [21]. Based on scanning tunneling microscopy (STM) work, Co was reported to grow in a homogeneous, quasilayer-by-layer mode up to 3 AL with hexagonal stacking on Pt(111) [22]. A large Co/Pt interface anisotropy per unit area of  $105$  mJ/m<sup>2</sup> [24] gives rise to a strong uniaxial perpendicular anisotropy  $K_{u,1} \sim 2.7$  MJ/m<sup>3</sup> at 0.6 nm Co thickness. Consistently large values of the second order anisotropy constant  $K_{u,2} \sim 0.20$  MJ/m<sup>3</sup> confirm the presence of hexagonal hcp (0001) Co, in agreement with the aforementioned STM studies [22,23].

Figure 1 shows a schematic diagram of the present wedge structure together with two representative polar Kerr hysteresis loops measured at two positions corresponding to  $t_{Ru} = 0.3$  (large field slope) and 1 nm, respectively, on the Ru wedge. The Kerr system uses a He-Ne laser ( $\lambda = 633$  nm) with 0.8 mm spot size, and the 20 mm wide sample is translated in front of the beam in 250  $\mu\text{m}$  steps, resulting in a thickness resolution of better than 0.1 nm or half an atomic layer of Ru ( $d_{0001}^{\text{bulk}} = 0.214$  nm, slope of Ru wedge is 0.1 nm per mm). Extended averaging and low noise differential detection allow measurements of the polar Kerr angle,  $\theta_K$ , with a precision of better than 0.1 mdeg in external magnetic fields up to 2 T aligned normal to the film plane [25]. The Kerr loops were generally square with close to 100% remanence and coercivities  $H_C$  in the range 80–120 kA/m. A detailed investigation of the anisotropy constants  $K_{u,1}$  and  $K_{u,2}$  as a function of the Ru thickness  $t_{Ru}$  did not reveal much structure, except for a slight increase of  $K_{u,1} = 2.7\text{--}2.9$  MJ/m<sup>3</sup> as  $t_{Ru}$  increases. Quite dramatic effects, however, are observed in the Kerr rotation, which we analyze as follows:

$$\theta_K(H) = \theta_S + \theta_P(H) = \theta_S + \chi^{\text{Kerr}} H. \quad (1)$$

Here,  $\theta_S$  is the saturation Kerr angle obtained by linear extrapolation from high field to  $H = 0$  and  $\theta_P(H)$  is the paramagnetic Kerr angle, which can be character-

ized by the field independent *Kerr susceptibility*,  $\chi^{\text{Kerr}}$ . Figure 2 shows experimental results of  $\theta_S$  and  $\chi^{\text{Kerr}}$  as a function of  $t_{Ru}$ .  $\theta_S$  is of the order of 20 mdeg and shows an overall monotonic and roughly linear decline of  $\sim 1.5$  mdeg/nm as  $t_{Ru}$  increases, in line with what one expects if Ru is assumed to attenuate the ferromagnetic signal from Co. Superimposed on this decline is a weak modulation of about (1–2)%, that we turn to later. Much stronger modulation amplitudes are observed in  $\chi^{\text{Kerr}}$ , which was determined in the field range  $0.2 < H < 1.7$  T using linear regression, and is shown in Fig. 2(b). The presently observed susceptibility translates into a field-induced Kerr angle  $\theta_P \sim 3$  mdeg at 1.5 T or about 15% of  $\theta_S$ , which is 3 times larger than the modulation amplitude of about 5% reported previously by Suzuki *et al.* [3,4] at such fields [27] in Fe/Ag,Au/Fe systems. Clearly two strong susceptibility peaks appear at 0.35 and 1.57 nm Ru thickness, yielding a peak separation of  $\sim 1.2$  nm. In addition to this long period behavior we resolve much finer, rapid oscillations of the order of 0.1–0.3 nm around the main peaks. These ultrashort period components are clearly out of the error bar of the measurement and have also been observed in other NM/Co overlayer systems including NM = Cu, Pd, Pt, Ir, and Rh. The simultaneously monitored reflectivity did not correlate with either the long or short period oscilla-

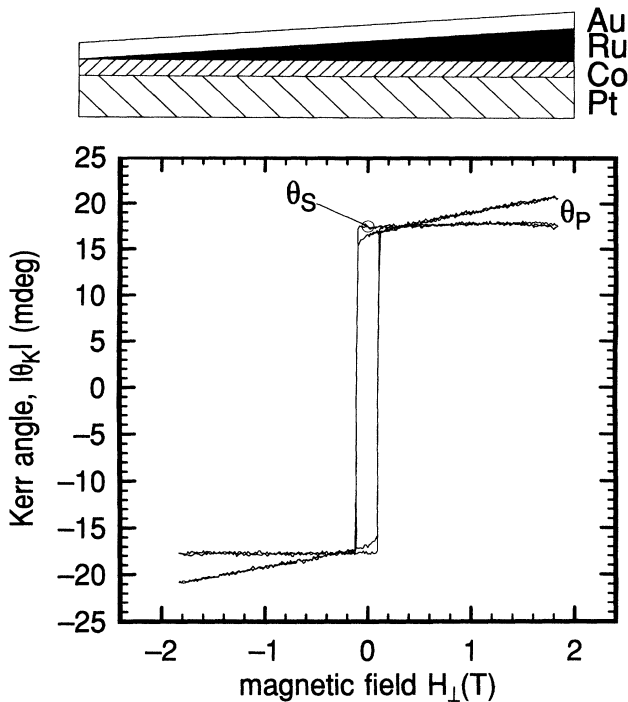


FIG. 1. Schematic diagram of the present Co/Ru overlayer wedge structure and two representative polar MOKE hysteresis loops taken at different wedge positions, corresponding to 0.3 and 1 nm Ru thickness, respectively (see Fig. 2). The saturation Kerr angle  $\theta_S$  and the field-induced contribution  $\theta_P$  according to Eq. (1) are analyzed.

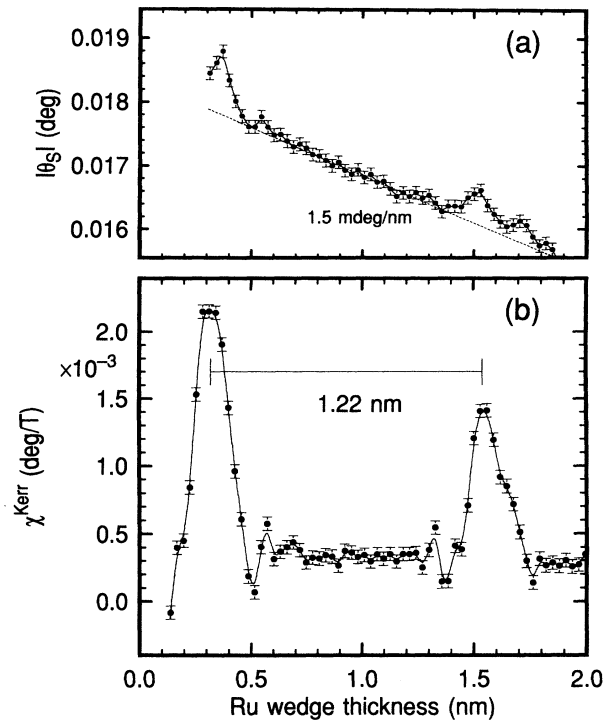


FIG. 2. (a) Saturation Kerr angle,  $\theta_S$ , and (b) Kerr susceptibility,  $\chi^{\text{Kerr}}$ , of the structure described in Fig. 1 as a function of the Ru wedge thickness. The lines represent spline functions through the data points.

tions, and optical interference or scattering mechanisms can therefore be ruled out as possible origin.

Before turning to the interpretation of  $\chi^{\text{Kerr}}$ , we first establish its relationship to exchange coupling between two Co layers *across* Ru. The period of 1.2 nm coincides with published results on in-plane, (0001) textured Co/Ru multilayers [5] and out-of-plane epitaxial Co/Ru(0001) superlattices [28]. Figure 3 shows selected perpendicular hysteresis loops as a function of  $t_{\text{Ru}}$  of one of the present Co/Ru-wedge/Co sandwich structures. The thin ( $d_{\text{Ru}} \leq 0.3$  nm) and thick ( $d_{\text{Ru}} \sim 1.7$  nm) end of the wedge are clearly ferromagnetically coupled and show close to 100% remanence. In the thickness range  $0.3 < d_{\text{Ru}} < 1.7$  nm, the remanent Kerr angle drops and reaches its minimum at about 1.1 nm, which we identify as the thickness of maximum antiferromagnetic (AF) coupling strength  $J_{\text{AF}}$ . The respective saturation field,  $H_{\text{sat}}^{\perp} = -(4J_{\text{AF}}/M_S + H_K)$  [28], exceeds the maximum available field strength of 2 T, so that a quantitative determination of  $J_{\text{AF}}$  was not possible.  $H_K$  is the effective anisotropy field which was determined to be  $\sim 1.8$  T. Nevertheless, as, e.g., indicated by the loop near  $t_{\text{Ru}} = 1.5$  nm, AF coupling is clearly present, and we can use the remanent Kerr angle to determine its periodicity. We estimate an AF-FM peak distance of 0.7 nm or a period of  $\sim 1.4$  nm. This is consistent within an estimated thickness error bar of  $\pm 0.1$  nm with the peak separation found in  $\chi^{\text{Kerr}}$ , thus emphasizing the close connection between both quantities. Furthermore, both effects have the same phase. The appearance of  $\chi^{\text{Kerr}}$  peaks coincides with FM coupling, and their absence apparently leads to AF coupling. Note finally the overall decay of 1.5 mdeg/nm, identical to the one in Fig. 2(a).

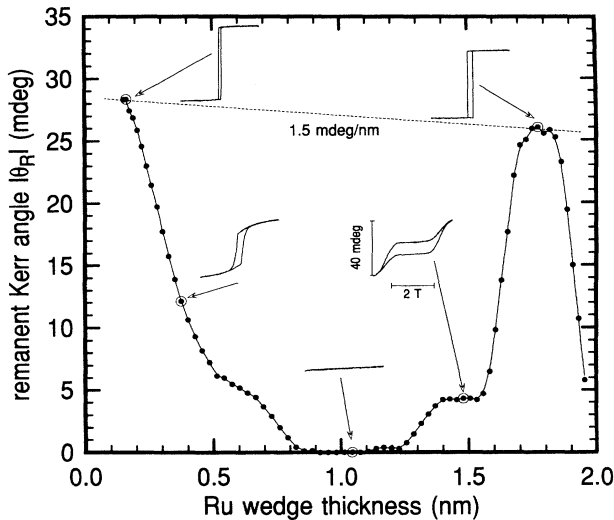


FIG. 3. Remanent polar Kerr angle,  $\theta_R$ , of a Co(0.6 nm)/Ru-wedge/Co(0.6 nm) sandwich structure as a function of the Ru wedge thickness. Representative Kerr loops indicate AF perpendicular alignment of the two Co layers at  $d_{\text{Ru}} \sim 1.1$  nm Ru. A period of  $\sim 1.4$  nm is estimated.

The polar Kerr rotation is a linear combination of the real and imaginary parts of the complex frequency dependent diagonal and off-diagonal conductivity tensor elements  $\tilde{\sigma}_{xx}(\omega)$  and  $\tilde{\sigma}_{xy}(\omega)$ , respectively [19]:  $\theta_K = \text{Im}\{\tilde{\sigma}_{xy}/i\tilde{n}\tilde{\sigma}_{xx}\}$ . To explain the presently observed paramagnetic Kerr effect,  $\theta_P$ , the phenomenological intraband Kerr effect theory of free electrons in a magnetic material can be adapted [19,29,30]. Here  $\tilde{\sigma}_{xy}^P(\omega)$  is proportional to the free electron spin polarization  $\langle\sigma_{\text{free}}\rangle = (N_{\uparrow} - N_{\downarrow})/(N_{\uparrow} + N_{\downarrow})$ , which in Pauli paramagnets like Ru is induced by Zeeman splitting of free electrons at the Fermi level.  $N = N_{\uparrow} + N_{\downarrow}$  is the volume density of (up and down spin) free electrons [29,30]. For (small) fields  $H$ , in the range of several tesla ( $g\mu_B H \ll \epsilon_F$ ),  $\tilde{\sigma}_{xy}^P(\omega)$  and therefore  $\theta_P$  can be expressed in terms of the Pauli paramagnetic susceptibility of free electrons, which relates the (volume) magnetization density  $M = -\mu_B N \langle\sigma_{\text{free}}\rangle$  to the external field  $H$ ,  $M = \chi^{\text{Pauli}} H$ . According to Ref. [30] we write

$$\theta_P \rightarrow \tilde{\sigma}_{xy}^P = -\frac{\omega_p^2 \epsilon_0}{\mu_B N} [A + B] \chi^{\text{Pauli}} H$$

with

$$A = -\frac{\Omega}{\Omega^2 + (\gamma + i\omega)^2}, \quad (2)$$

$$B = \frac{|P_0|}{ev_0} \left(1 - \frac{i\omega(\gamma + i\omega)}{\Omega^2 + (\gamma + i\omega)^2}\right),$$

where  $\omega_p$  is the plasma frequency of free carriers ( $\omega_p^2 = Ne^2/m^* \epsilon_0$ ),  $|P_0|$  is the maximum value of the dipole moment  $\mathbf{P}(\mathbf{k})$  per unit cell due to spin orbit coupling,  $v_0$  is the Fermi velocity,  $\gamma$  is the inverse of the free electron lifetime (damping), and  $\Omega$  is the inverse lifetime due to skew scattering, all of which are field independent quantities. Therefore, at any given photon energy  $E_{\text{ph}} = \hbar\omega$ , the presently measured Kerr susceptibility is directly proportional to the Pauli paramagnetic susceptibility or the free electron density of states at the Fermi level,  $N(\epsilon_F)$ ,

$$\chi^{\text{Kerr}} = C \chi^{\text{Pauli}} = C \mu_B^2 N(\epsilon_F). \quad (3)$$

The proportionality constant  $C$  contains, besides the factors discussed in Eq. (2), also a complicated function of the optical constants  $n$  and  $k$  [19], which are contained in  $\tilde{n}$  and  $\tilde{\sigma}_{xx}$  as indicated above. We estimate a typical size  $C \sim 10^3$  deg/ $\mu_B$ , which means that extremely small paramagnetic moments of typically only  $10^{-5} \mu_B$  (per tesla) lead to sizable Kerr effects  $\theta_P \sim 10$  mdeg for thick films and  $\theta_P \sim 1$  mdeg for the present ultrathin films. In view of the above result, we can now interpret the Kerr susceptibility data in Fig. 2(b) as direct evidence for the presence of charge (spin) density waves or quantum well (QW) resonance states at the Fermi level of Ru. The observation of peak widths (FWHM) of only  $\sim 1$  AL in  $\chi^{\text{Kerr}}$ , in particular, points to the presence of sharp QW resonances. The additional fine structure near the main peaks is not fully understood. It could be related to the subtle interplay between the factors entering the constant  $C$  (damping  $\gamma$ , skew scattering frequency  $\Omega$ ) in Eq. (3) and  $N(\epsilon_F)$ , which may both depend on the thickness  $t_{\text{Ru}}$ . Steplike roughness due

to layer-by-layer growth appears unlikely, since that should result in continuous monolayer oscillations along the entire length of the wedge, which we do not observe.

Returning to the field independent saturation Kerr angle,  $\theta_S$ , discussed in Fig. 2(a), we emphasize that this is mainly due to interband transitions between exchange split Co  $d$  and  $p$  states. The appearance of peak features as a function of  $t_{\text{Ru}}$  indicates the presence of exchange split Ru  $4d$  states [26]. On the other hand, the existence of a one-to-one correlation between their position and relative magnitude with the much stronger  $\chi^{\text{Kerr}}$  features suggests a similar free electron origin. Stray fields,  $H_{\text{stray}}$ , due to local roughness in the perpendicularly magnetized single domain Co film, e.g., could induce Zeeman splitting of Ru  $s$  and  $p$  levels. Since stray fields switch with the Co magnetization, they will not appear in  $\chi^{\text{Kerr}}$  but will just offset  $\theta_S$ .  $H_{\text{stray}} \sim 0.4$  T would be required to produce the observed peak features in  $\theta_S$ , if no other mechanisms were present. In principle though,  $\theta_S$  is composed of at least three components,  $\theta_S = \theta_S^{\text{Co}} + \theta_{\text{exchange}}^{\text{Ru}} + \theta_{\text{stray}}^{\text{Ru}}$ , which cannot easily be separated from one another. Nevertheless, it should be possible to distinguish between *magnetic* spin density and *nonmagnetic* charge density waves, i.e., magnetic and nonmagnetic QW states, by separate analysis of  $\theta_S$  and  $\chi^{\text{Kerr}}$ .

In summary, we have demonstrated that field dependent polar MOKE measurements are a sensitive probe of free electrons at the Fermi surface of ultrathin paramagnet/ferromagnet metal structures. These effects are quite strong in Ru, show the same periodicity as exchange coupling oscillations as a function of the Ru thickness, and can conveniently be used to study the electronic underpinnings of indirect exchange coupling phenomena. Such measurements are not necessarily restricted to the use of perpendicularly oriented samples and/or the polar geometry.

We gratefully acknowledge discussions with C. Chappert, G. R. Harp, F. Herman, B. A. Jones, S. S. P. Parkin, J. C. Scott, and J. Stöhr. One of us (A. C.) would like to thank the Alexander von Humboldt foundation for continuous support.

- [1] Y. Suzuki, T. Katayama, S. Yoshida, K. Tanaka, and K. Sato, Phys. Rev. Lett. **68**, 3355 (1992).
- [2] W. R. Bennett, W. Schwarzacher, and W. F. Egelhoff, Jr., Phys. Rev. Lett. **65**, 3169 (1990).
- [3] Y. Suzuki and T. Katayama, Mater. Res. Soc. Symp. Proc. **313**, 153 (1993).
- [4] T. Katayama, Y. Suzuki, M. Hayashi, and A. Thiaville, J. Magn. Magn. Mater. **126**, 527 (1993).
- [5] S. S. P. Parkin, N. More, and K. P. Roche, Phys. Rev. Lett. **64**, 2304 (1990); S. S. P. Parkin, R. Bhadra, and K. P. Roche, Phys. Rev. Lett. **66**, 2152 (1991).
- [6] S. S. P. Parkin, Phys. Rev. Lett. **67**, 3598 (1991).
- [7] A. Fuss, S. Democritov, P. Grünberg, and W. Zinn, J. Magn. Magn. Mater. **103**, L221 (1992); J. Unguris, R. J. Celotta, and D. Pierce (to be published); M. T. Johnson, S. T. Purcell, N. W. E. McGee, R. Coehoorn, J. aan de Stegge, and W. Hoving, Phys. Rev. Lett. **68**, 2688 (1992); P. J. H. Bloemen, R. van Dalen, W. J. M. de Jonge, M. T. Johnson, and J. aan de Stegge, J. Appl. Phys. **73**, 5972 (1993).
- [8] M. T. Johnson, R. Coehoorn, J. J. de Vries, N. W. E. McGee, J. aan de Stegge, and P. J. H. Bloemen, Phys. Rev. Lett. **69**, 969 (1992).
- [9] A. Schreyer, K. Bröhl, J. F. Ankner, Th. Zeidler, P. Bödeker, N. Metoki, C. F. Maikrzak, and H. Zabel, Phys. Rev. B **47**, 15334 (1993); M. A. Howson, B. J. Hickey, J. Xu, D. Grieg, and N. Wisser, Phys. Rev. B **48**, 1322 (1993).
- [10] V. Grolier, D. Renard, B. Bartenlian, P. Beauvillain, C. Chappert, C. Dupas, J. Ferré, M. Galtier, E. Kolb, M. Mulloy, J. P. Renard, and P. Veillet, Phys. Rev. Lett. **71**, 3023 (1993); S. S. P. Parkin, R. F. C. Farrow, R. F. Marks, A. Cebollada, G. R. Harp, and R. J. Savoy, Phys. Rev. Lett. **72**, 3718 (1994).
- [11] P. Bruno and C. Chappert, Phys. Rev. Lett. **67**, 1602 (1991); Phys. Rev. Lett. **67**, 2592 (1991); P. Bruno, Phys. Rev. B **46**, 261 (1992).
- [12] D. M. Edwards and J. Mathon, J. Magn. Magn. Mater. **93**, 85 (1991).
- [13] B. A. Jones and C. B. Hanna, Phys. Rev. Lett. **71**, 4253 (1993); see also comment by P. Bruno, Phys. Rev. Lett. **72**, 3627 (1994) and reply by C. B. Hanna and B. A. Jones, *ibid.* p. 3628.
- [14] M. D. Stiles, Phys. Rev. B **48**, 7238 (1993).
- [15] E. Bruno and B. L. Gyorffy, J. Phys. Condens. Matter **5**, 2109 (1993).
- [16] J. E. Ortega and F. J. Himpsel, Phys. Rev. Lett. **69**, 844 (1992); J. E. Ortega, F. J. Himpsel, G. J. Mankey, and R. F. Willis, Phys. Rev. B **47**, 1540 (1993).
- [17] C. Carbone, E. Vescovo, O. Rader, W. Gudat, and W. Eberhardt, Phys. Rev. Lett. **71**, 2805 (1993).
- [18] S. E. Schnatterly, Phys. Rev. **183**, 664 (1969).
- [19] W. Reim and J. Schoenes, in *Handbook on Ferromagnetic Materials*, 5, 133-236 (1990).
- [20] T. C. Huang (private communication).
- [21] M. F. Toney (private communication).
- [22] P. Grütter and U. T. Dürig, Phys. Rev. B **49**, 2021 (1994).
- [23] The structure of ultrathin Co depends sensitively on the cap layer. Co films sandwiched between Pt reveal cubic fcc (111) rather than hcp (0001) orientation [24].
- [24] D. Weller, A. Carl, M. F. Toney, and C. Chappert (to be published).
- [25] D. Weller, Y. Wu, J. Stöhr, M. G. Samant, B. D. Hermsmeier, and C. Chappert, Phys. Rev. B **49**, 12888 (1994).
- [26] G. R. Harp, S. S. P. Parkin, W. L. O'Brien, and B. P. Tonner, J. Appl. Phys. **76**, 6471 (1994).
- [27] Y. Suzuki (private communication).
- [28] K. Ounadjela, D. Muller, A. Dinia, A. Arbaoui, P. Panissod, and G. Suran, Phys. Rev. B **45**, 7768 (1992).
- [29] J. L. Erskine and E. A. Stern, Phys. Rev. B **8**, 1239 (1973).
- [30] J. Schoenes, in *Materials Science and Technology*, edited by R. W. Cahn, P. Haasen, and E. J. Kramer (VCH, 1991), Vol. 3; W. Reim, O. E. Hüsser, J. Schoenes, E. Kaldis, P. Wachter, and K. Seiler, J. Appl. Phys. **55**, 2155 (1984).